Title

Direct Amination of Alcohols Catalyzed by Aluminum Triflate: An Experimental and Computational Study

Journal

Chemistry - A European Journal, 24(53)

ISSN

0947-6539

Authors

Payard, Pierre-Adrien
Gu, Qingyi
Guo, Wenping
et al.

Publication Date

2018-09-20

DOI

10.1002/chem.201801492

Peer reviewed

Direct Amination of Alcohols Catalyzed by Aluminum Triflate: an Experimental and Computational Study

Pierre-Adrien Payard,[a,b] Qingyi Gu,[a] Wenping Guo,[a,c] Qianran Wang,[a] Matthieu Corbet,[a] Carine Michel,[c] Philippe Sautet,[c,d] Laurence Grimaud,[b] Raphael Wischert,[a]* and Marc Pera-Titus[a]*

Abstract: Among the best performing homogeneous catalysts for the direct amination of activated secondary alcohols using electron-poor amine derivatives, metal triflates, such as aluminum triflate, $Al(OTf)_3$, stand out. Here we report the extension of this reaction to electron-rich amines and activated primary alcohols, and provide detailed insight into the structure and reactivity of the catalyst under working conditions in both nitromethane and toluene solvent, through experiment (cyclic voltammetry, conductimetry, NMR), and density functional theory (DFT) simulations. Competition between aniline and benzyl alcohol is found to be critical for explaining how the solvent conditions the reactivity. The catalyst structures predicted from calculations are validated by the experiments. While a S_N1-type mechanism is active in nitromethane, we propose a S_N2 mechanism in toluene, thus rationalizing the much higher selectivity when using this solvent. Also, unlike what is commonly assumed in homogeneous catalysis, we show that different active species may be active instead of only one.

Introduction

Amines hold a substantial place among the intermediates used and synthesized by the chemical industry, with a vast repertoire of applications.[1] Among the different methods for amine synthesis, the direct amination of alcohols constitutes an attractive transformation, since alcohols (including biomass-derived alcohols) are readily available, easy to handle and water is generated as sole byproduct.[2] Unlike traditional pre-activation methods which require transformation of the OH-group into leaving groups such as halides, carboxylates, phosphates or carbonates, this synthetic approach is consistent with the principles of green chemistry, both in terms of atom economy and waste prevention.[3]

During the last decades, three main strategies have emerged for the direct amination of alcohols: (i) the borrowing hydrogen methodology (BH_2) using either Ru or Ir complexes,[4] and more recently non-noble metal complexes based on Mn[5] or Fe,[6] (ii) Tsuji-Trost type reactions for allylic alcohols using Pd[7] or Ni[7a, 8] complexes, and (iii) Lewis-acid catalysis based on a variety of salts and ligands.[2a, 2d] The latter is attractive as it uses non-noble metal, inexpensive, and low-toxic salts. Among the best performing catalysts, triflates and triflimides stand out as Lewis superacids.[9] Metal triflates and triflimides, based on Ca,[10] Al,[11] In,[12] Yb,[13] La,[13c] Hf,[13c] Bi,[14] Cu,[15] Ag,[16] Hg,[17] and Au,[18] including the parent triflic acid (HOTf),[19] were found active for a broad range of acid-catalyzed reactions. In particular, Mashima and coworkers reported $Al(OTf)_3$ as a powerful catalyst for the amination of secondary allylic or benzylic alcohols.[11b] The reaction proceeded to completion and with high selectivity in nitromethane at mild temperature (25-50 °C) and short reaction times (from 5 min to 6 h, typically 10-30 min). However, as a major drawback, the reaction scope was limited to electron-poor amine derivatives, such as amides, sulfonamides, carbamates, and to activated alcohols (Scheme 1, left).[11b]

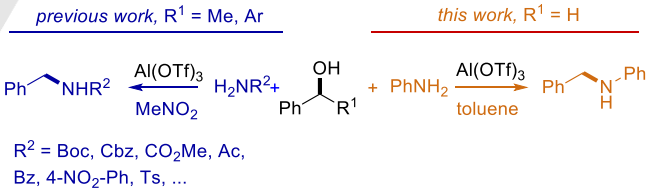

Scheme 1. Scope of the direct amination of alcohols catalyzed by $Al(OTf)_3$.[11b]

With respect to the catalytic mechanism, there is general consensus that substitution of OH-groups with C-, S-, and O-nucleophiles proceeds *via* a S_N1-type mechanism, in the presence of hard Lewis or Brønsted acids.[2a, 2d] Carbocation intermediates are generated by coordination of the alcohol to the acidic center, and subsequent formation of an acid-OH^- species. Racemization of optically active alcohols,[2d] and electronic and solvent effects support such a mechanism. Due to their polar nature, solvents typically used for S_N1-type reactions, such as dichloromethane,[10] dioxane,[14b, 19] nitromethane,[11b, 13a, 16b] and water,[12, 14a] can stabilize ionic intermediates. Additives such as KPF_6 for $Bi(OTf)_3$[14b] and Bu_4NPF_6 for $Ca(NTf_2)_2$[10] can enhance the catalytic performance, most likely by generating more active species by exchange of TfO^- and NTf_2^- anions for PF_6^-.

[a] P-A. Payard, Q. Gu, Dr. W. Guo, Q. Wang, Dr. M. Corbet, Dr. R. Wischert, Dr. M. Pera-Titus
Eco-Efficient Products and Processes Laboratory (E2P2L), UMI 3464 CNRS – Solvay, 3966 Jin Du Road, Xin Zhuang Ind. Zone, 201108 Shanghai (China).
E-mail: raphael.wischert@solvay.com, marc.pera-titus-ext@solvay.com

[b] P-A. Payard, Dr. L. Grimaud
PASTEUR, Département de chimie, École normale supérieure, PSL Research University, Sorbonne Universités, UPMC Univ. Paris 06, CNRS 75005 Paris (France).

[c] Dr. C. Michel. Dr. W. Guo
Univ. Lyon, ENS de Lyon, CNRS UMR 5182, Université Claude Bernard Lyon 1, Laboratoire de Chimie, F69342, Lyon (France).

[d] Prof. P. Sautet
Department of Chemical and Biomolecular Engineering and department of Chemistry and Biochemistry, University of California, Los Angeles, California, 90095 (USA).

Present addresses:
W. Guo
National Energy Center for Coal to Liquids, Synfuels China Co., Ltd, Huairou District, Beijing 101400 (China).

Supporting information for this article is given via a link at the end of the document.

While a S_N1-type mechanism appears to be predominant for a large majority of metal triflates, key aspects of the Lewis acid-catalyzed amination reaction of alcohols remain unclear. This lack of understanding can be certainly ascribed to the difficult access to the catalyst structure under working conditions. Indeed, detailed structural and spectroscopic data on metal triflates is scarce, in particular in solution, with the notable exception of recent ESI-MS[9, 20] and NMR studies[21] reported by Duñach, Gal and coworkers. Likewise, few theoretical investigations of metal triflate-catalyzed reactions of alcohols[22] or ethers[22b, 23] exist. As a measure of Lewis acidity, the effective charge density (*i.e.* the ratio between the DFT-calculated cation charge and the effective ionic radius) was found to correlate with the catalytic activity for the C-O bond cleavage of ethers.[22b, 23] Here, we extend the direct amination of alcohols catalyzed by $Al(OTf)_3$ to electron-rich amines and primary benzylic alcohols, using the reaction between benzyl alcohol (BnOH) and aniline as a model system (Scheme 1, right). We show that the selectivity of the reaction strongly depends on the choice of the solvent, with an unexpectedly favourable outcome in toluene, a solvent typically not used for this class of reactions. We then provide detailed insight into the structure of the catalyst under working conditions, using different analytical methods. DFT calculations are performed to rationalize the findings and the reaction mechanism.

Results and Discussion

Amination reaction in nitromethane and toluene

First, we investigated the catalytic properties of $Al(OTf)_3$ in nitromethane, a polar solvent typically used for metal triflate-catalyzed reactions.[11b] For this purpose, a 1:2 mixture of benzyl alcohol (BnOH) and aniline was heated in the presence of a catalytic amount of $Al(OTf)_3$ (Scheme 2). Unlike the results reported by Mashima and coworkers obtained with electron-poor amine derivatives and secondary allylic or benzylic alcohols,[11b] our reaction required very harsh conditions. Indeed, even at 160 °C under microwave irradiation, the primary amination product *N*-phenylbenzylamine (**3**) was obtained with poor selectivity (Table 1, entry 1). Besides, the carbon balance turned out to be low, most likely due to the formation of oligomers. Lower temperatures did not lead to any product.

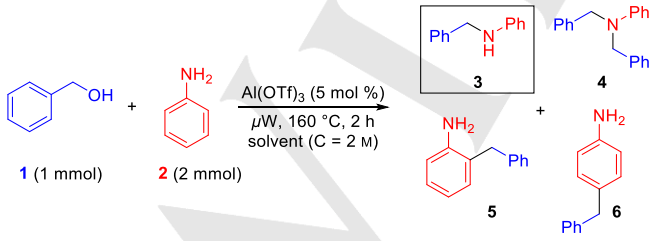

Scheme 2. Main products obtained in the amination reaction of benzyl alcohol (**1**, BnOH) with aniline (**2**).

Unexpectedly, when the reaction was performed under the same conditions, but in toluene, a non-polar solvent, the expected product **3** was obtained with high selectivity (90%) and fair yield (Table 1, entry 2), and an almost quantitative carbon balance was achieved. Note, that in both solvents only trace amounts of the secondary amine **4** and Friedel-Crafts products **5-6** were formed. Less byproduct was again observed in toluene.

The markedly different reaction outcome for nitromethane and toluene suggests different mechanisms. Therefore, to better understand the different reactivity in both solvents and the need of much higher temperature, compared to electron-poor amines and activated secondary alcohols, a dedicated mechanistic study of the $Al(OTf)_3$-catalyzed amination reaction was undertaken in both nitromethane and toluene.

Table 1. Conversion of benzyl alcohol, (BnOH, **1**), yields, and carbon balance (in %) for the reaction with aniline in two different solvents, according to Scheme 2. Values obtained by GC analysis, using biphenyl as an internal standard.

Solvent	Conv.	Yield				Carbon balance
	1	**3**	**4**	**5**	**6**	
Nitromethane	63	26 (41)[a]	1.2	2.9	2.2	59
Toluene	41	37 (90)[a]	0.3	1.1	0.8	96

a) Selectivity to *N*-phenylbenzylamine (**3**).

Nature of $Al(OTf)_3$ in nitromethane and coordination of benzyl alcohol

The nature of $Al(OTf)_3$ was first investigated in nitromethane by different analytical methods (cyclic voltammetry, conductimetry, ^1H- and ^{13}C-NMR spectroscopy). Cyclic voltammetry (CV) allows the characterization of redox-active species by their oxidation and reduction potentials. In this technique, the reactivity can be assessed by considering that the reduction or oxidation currents are proportional to the concentration of the electroactive species.[24] The CV of $Al(OTf)_3$ dissolved in nitromethane (10 mM) exhibited two non-reversible reduction peaks (i.e. R_1 and R_2) centered at -0.55 V and -0.95 V *vs.* SCE, respectively (Figure 1a). An increase of the scan rate up to 2 Vs^{-1} modified the relative intensity between both peak currents (Figure S1). Such a behavior can be typically ascribed to the existence of an equilibrium between two different species.

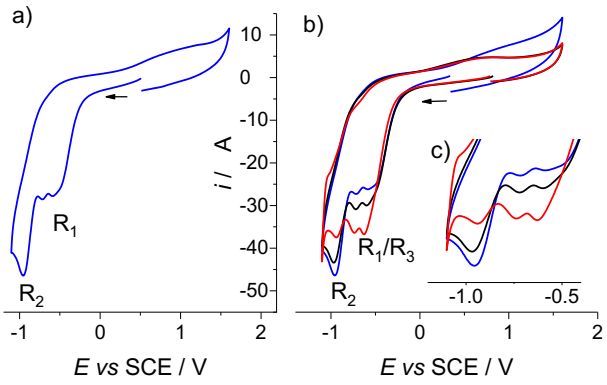

Figure 1. CV towards reduction potentials recorded on a steady glassy carbon disk electrode (d = 1 mm) in nitromethane containing *n*-Bu_4NBF_4 (300 mM) at 20 °C with a scan rate of 0.5 V s^{-1}. a) $Al(OTf)_3$ (10 mM); b) $Al(OTf)_3$ upon addition of increasing amounts of BnOH (0 [in blue], 11 [in black] and 50 equiv [in red]); and c) insert of b).

The addition of water increased the reduction peak current at R_1 at the expense of peak R_2 (Figure S2). The reduction peak R_1 could thus be attributed to water coordinated to $Al(OTf)_3$, while peak R_2 could be attributed to nitromethane coordinated to $Al(OTf)_3$.[25] A similar reduction pattern for nitromethane was observed in the presence of various Lewis acids such as $LiNTf_2$, $LiBF_4$ and $AlCl_3$ (Figure S3).

To assess any potential triflate dissociation, a series of conductivity measurements was performed in nitromethane at different $Al(OTf)_3$ concentrations. The conductivity of the parent solution was found to be very low and a plot of the conductivity *vs.* $Al(OTf)_3$ concentration is characteristic of poorly dissociated electrolytes (Figure 2, ▲). This observation is consistent with published reports establishing a weak dissociation of metal triflate salts in low-coordinating solvents such as nitromethane.[20] Additional CV experiments were conducted to investigate the coordination of BnOH to Al(III). The reduction peak R_2 decreased significantly upon BnOH addition (Figure 1b, c), whereas the current intensity increased at a reduction potential similar to R_1. This observation is likely due to the appearance of a new peak (R_3), which can be attributed to BnOH coordinated to $Al(OTf)_3$. This complex is expected to behave similarly to that formed with water (reduced at R_1), which could explain the similar reduction potentials. These results underline the high affinity of BnOH for Al(III), being able to displace nitromethane under conditions similar to those of the catalytic reaction. However, in analogy to water, coordination of BnOH does not result in the dissociation of the triflate ions, as apparent from the plot of conductivity *vs.* $Al(OTf)_3$ concentration in the presence of excess BnOH (100 mM) (see Figure 2, Δ).

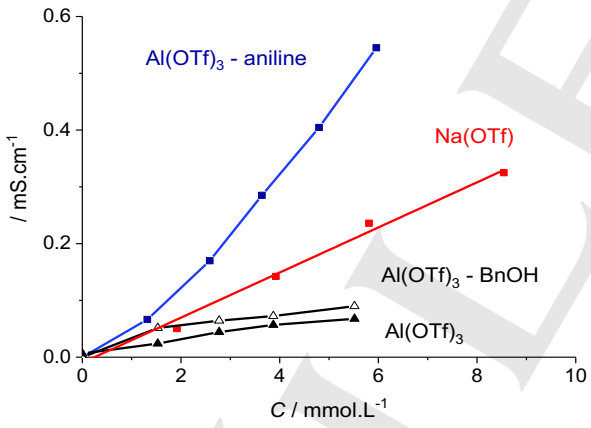

Figure 2. Conductivity of $Al(OTf)_3$ in nitromethane (▲), with excess BnOH (100 mM, Δ) and with excess aniline (100 mM, blue ■) as a function of the $Al(OTf)_3$ concentration. For comparison, the conductivity of NaOTf in nitromethane (red ■) is also plotted.

To gain more insight into the nature of the possible reaction intermediates, the complexes formed between BnOH and $Al(OTf)_3$ were analyzed by ^{1}H- and ^{13}C-NMR. In the presence of 10 equiv of $Al(OTf)_3$, the singlet at 4.63 ppm accounting for the two benzylic protons of BnOH was shifted to 4.64 ppm (Figure S4a). Comparable shifts were observed by ^{13}C-NMR, with all signals being shifted by about 0.5 ppm (Figure S4b, c). Even if tiny,[26] this shift is consistent with the coordination of BnOH to Al(III) and corresponds to a rapid equilibrium on the NMR timescale.

Catalyst deactivation by aniline in nitromethane

Upon addition up to 1.5 equiv of aniline to a solution of $Al(OTf)_3$, no free aniline was present, as evidenced by the absence of its characteristic oxidation peak at +1.0 V *vs.* SCE in the CV plot (Figure 3a). CV towards negative potentials exhibited a new reduction peak at -0.7 V *vs.* SCE (R_4), together with a markedly lower intensity of the reduction peak at -0.95 V (R_2) (Figure 3b). This observation is consistent with the formation of a complex between Al(III) and aniline.

Upon addition of 3 equiv of aniline (Figure 3a), the reduction peak at -1.0 V *vs.* SCE almost vanished. Moreover, the conductivity measured for $Al(OTf)_3$ with an aniline excess (100 mM) exhibited higher values than for a solution of sodium triflate, together with a linear-shaped curve that is consistent with the formation of ionic species (Figure 2, ■). *p*-Fluoroaniline was used as ^{19}F-NMR probe to study the complexation of aniline to Al(III). In the presence of 1 equiv of $Al(OTf)_3$, the ^{19}F-NMR signal shifted from -127 ppm to -110 ppm (fluorobenzene was used as an internal standard at -112 ppm). This shift confirms the coordination of aniline to Al(III), thus allowing the determination of the stoichiometry of the complex using the Job plot method (Figure S5). The point-shaped plot obtained is indicative of a large constant with a maximum observed at 0.6 corresponding to a 3:2 complex. The latter result is consistent with the CV curves, as free aniline was evidenced beyond 1.5 equiv of aniline with respect to $Al(OTf)_3$.

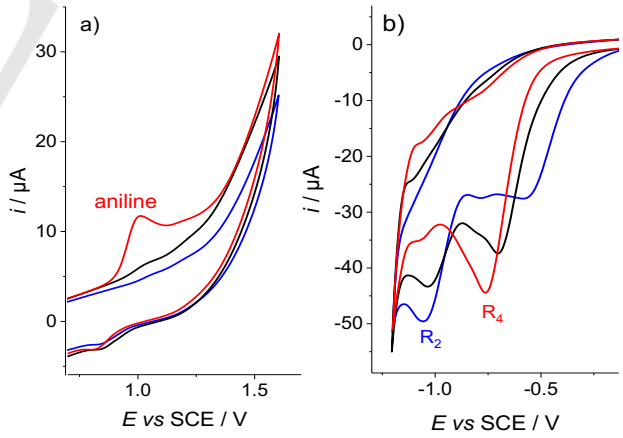

Figure 3. CV recorded on a steady carbon disk electrode (d = 1 mm) in nitromethane containing *n*-Bu_4NBF_4 (300 mM) at 20 °C and at a scan rate of 0.5 V s^{-1}. a) oxidation of $Al(OTf)_3$ (10 mM) with 1.5 equiv of aniline [blue], 1.6 equiv of aniline [black] and 1.8 equiv of aniline [red]; b) reduction of $Al(OTf)_3$ (10 mM) without aniline [blue], with 1 equiv of aniline [black] and 3 equiv of aniline [red].

To further rationalize the potential competition between BnOH and aniline, CV and NMR experiments were conducted in the presence of excess BnOH. All these tests confirm that aniline was able to displace BnOH from Al(III) (Figure S6, S7). Moreover, when 1-phenylethanol was reacted with electron-poor

p-tolylsulfonamide (2 equiv) at room temperature in the presence of 10%mol $Al(OTf)_3$ and aniline (2 equiv), no amination product was observed. Conversely, when the same reaction was performed under the very same conditions as in ref. [11b], but in the absence of aniline, the amination product was obtained (see Figure S8 and corresponding discussion in the supporting information). Overall, we can conclude that, in nitromethane, $Al(OTf)_3$ is deactivated by the formation of cationic complexes featuring aniline as ligand (Scheme 3a). Hence, BnOH is not expected to coordinate to Al(III), which is consistent with the poor selectivity observed under reaction conditions (see Table 1).

Competition between BnOH and aniline for Al in toluene

Next, we studied the coordination of BnOH and aniline to $Al(OTf)_3$ in toluene. $Al(OTf)_3$ alone proved to be insoluble in toluene. However, upon addition of 2 equiv of aniline, a single reduction plateau at $E_{1/2}$ = -0.5 V *vs.* SCE (R_5) was observed by CV, using a stationary method on an ultramicroelectrode.[27] Likewise, $Al(OTf)_3$ with 10 equiv of BnOH exhibited a single reduction plateau at $E_{1/2}$ = -1.0 V *vs.* SCE (R_6) (Figure 4). When 20 equiv of aniline were added to a solution of $Al(OTf)_3$ (10 mM) and 10 equiv of BnOH, two reduction plateaus associated with BnOH- and aniline-ligated Al(III), respectively, were observed. Still, the equilibrium was in favor of the BnOH complex and up to 80 equiv of aniline were necessary to fully shift the equilibrium towards coordinated aniline (Figure 4). Note, that this situation contrasts with the BnOH and aniline coordination pattern in nitromethane (*vide supra*).

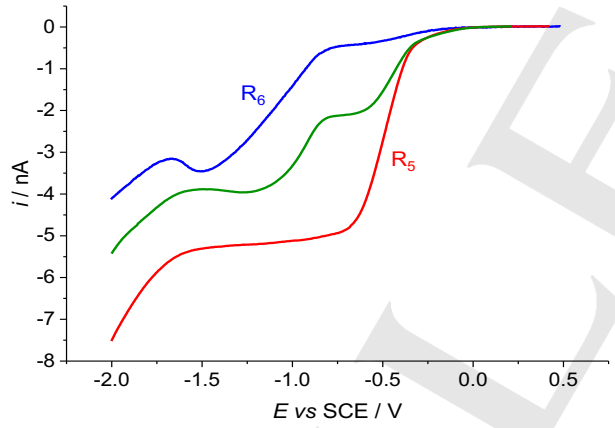

Figure 4. CV recorded on a steady gold ultramicroelectrode (d = 25 µm) in toluene containing *n*-hex_4NBF_4 (60 mM) at 20 °C with a scan rate of 0.01 V s^{-1}. From top to bottom: complexation of $Al(OTf)_3$ (10 mM) with 10 equiv of BnOH (blue), 10 equiv of BnOH and 30 equiv of aniline (green), and 10 equiv of BnOH and 80 equiv of aniline (red).

The competition between BnOH and aniline was further confirmed by ^{19}F-NMR spectroscopy, using *p*-fluoroaniline. In the presence of 5 equiv of *p*-fluoroaniline, $Al(OTf)_3$ was not soluble in toluene and this situation persisted even up to 40 equiv of *p*-fluoroaniline. From the integration of the *p*-fluoroaniline signal, it appeared that 1 equiv of *p*-fluoroaniline was coordinated to a non-soluble Al(III)-complex. In contrast, in the presence of excess BnOH (30 equiv), $Al(OTf)_3$ (2 mM) was completely soluble in toluene, as evidenced by the integration of the signal at -78 ppm for ligated triflates. This behavior does not exclude, however, a competition between BnOH and *p*-fluoroaniline under catalytic conditions. Indeed, when both BnOH and *p*-fluoroaniline were in excess with respect to $Al(OTf)_3$, the *p*-fluoroaniline signal in ^{19}F NMR shifted from -127 ppm to -121 ppm, proving that a significant quantity of *p*-fluoroaniline was ligated to Al(III).

Overall, the above results point out that the nature of $Al(OTf)_3$ under catalytic conditions depends to an important extent on the polarity of the solvent. While polar solvents such as nitromethane favor its dissociation and accordingly the coordination with electron-rich ligands such as aniline, no charged species are formed in the presence of non-polar solvents such as toluene (Scheme 3b). In this view, it is reasonable to expect a different catalytic mechanism as a function of the solvent. In particular, a S_N1-type mechanism seems very unlikely in toluene.

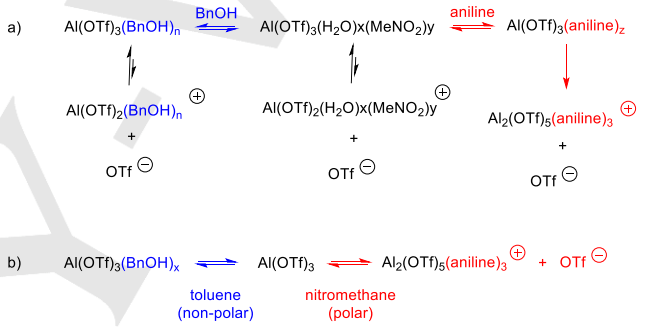

Scheme 3. a) Deactivation of $Al(OTf)_3$ in the presence of aniline in nitromethane by the formation of ionic complexes, b) simplified coordination pattern of $Al(OTf)_3$ complexes in toluene and nitromethane under catalytic conditions.

Determination of the structure of the catalyst by DFT calculations

To validate the experimental findings, interpret them in detail and provide mechanistic insight, we performed a DFT study, focusing on the surprisingly selective amination reaction in toluene. Calculations were performed at the B3LYP-D3(BJ) / def2-TZVP (COSMO) // BP86-D3(BJ) / def2-SV(P) level (see the supporting information for details, and validation of the method against CCSD(T) reference calculations, Tables S1 and S2).

$Al(OTf)_3$ can coordinate up to three additional ligands, assuming monodentate coordination of the triflate anions (as opposed to the bidentate κ^2-coordination in free $Al(OTf)_3$, Figure 5a). The binding free energy (ΔG_{bind}) of *n* ligands L to $Al(OTf)_3$ is defined as the free energy associated with the formation of a $[Al(OTf)_3L_n]$ complex from $Al(OTf)_3$ and *n* ligands L. At 25 °C in toluene this binding for a single ligand is strongest for BnOH (ΔG_{bind} = -87 kJ mol^{-1}), followed by aniline (ΔG_{bind} = -75 kJ mol^{-1}) and the reaction products, N-phenylbenzylamine (G_{bind} = -72 kJ mol^{-1}) and water (ΔG_{bind} = -70 kJ mol^{-1}) (Figure 5b-e and Table S3, entries 1-4). These values agree well with the experimentally observed stronger binding of BnOH compared to aniline (*vide supra*). Note, that alcoholysis of $Al(OTf)_3$ by BnOH, leading to the formation of $Al(OTf)_2(BnO)$ and HOTf, was found to be much

less favorable than binding of BnOH to Al(III) (ΔG = +32 *vs.* ΔG_{bind} = -87 kJ mol^{-1}, *vide supra*). The high affinity of BnOH for Al(III) can be rationalized *a priori* by the high oxophilicity of Al(III),[28] but it is possible to analyze more in detail the nature of the interaction by NBO charge analysis (Table 2): Both Al-O and Al-N bonds result mainly from ionic interactions, as apparent from charge separation (polarization) upon coordination. In the case of BnOH, the formal positive charge on Al(III) increases from +1.92 to +2.17, while the formal negative charge of the O of BnOH increases from -0.71 to -0.87, thus clearly demonstrating electron transfer from Al to O. For aniline coordination, while polarization of the N atom of aniline is comparable to that of the O atom of BnOH (-0.19 *vs.* -0.16, respectively), the effect on Al(III) is much smaller (+0.14 *vs.* +0.25 for BnOH). Also, the Al-O bond is much shorter than the Al-N bond, leading to a stronger coulombic interaction for the O atom. All these observations are consistent with a hard Lewis acid / hard Lewis base interaction, favoring O-coordination.

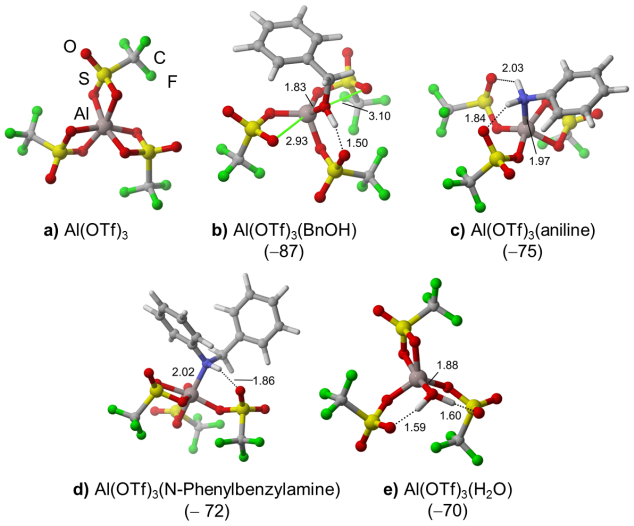

a) Al(OTf)$_3$ **b)** Al(OTf)$_3$(BnOH) (–87) **c)** Al(OTf)$_3$(aniline) (–75)

d) Al(OTf)$_3$(N-Phenylbenzylamine) (– 72) **e)** Al(OTf)$_3$(H$_2$O) (–70)

Figure 5. Optimized structures of a) free Al(OTf)$_3$, b-c) after coordination of reactants, d-e) after coordination of products, and calculated binding free energies (ΔG_{bind} at 25 °C in toluene, kJ mol^{-1}, indicated in brackets).

Table 2. Selected NBO partial charges estimated by NBO,[29] and Al-*O*(H)CH$_2$C$_5$H$_5$ and Al-*N*(H)$_2$C$_5$H$_5$ bond lengths for Al(OTf)$_3$, Al(OTf)$_3$(BnOH) and Al(OTf)$_3$(aniline). Changes, compared to free Al(OTf)$_3$, BnOH and aniline, are indicated in brackets.

	Al(OTf)$_3$	Al(OTf)$_3$(BnOH)	Al(OTf)$_3$(aniline)	BnOH	aniline
charge on Al	1.92	2.17 (+0.25)	2.06 (+0.14)		
charge O/N		-0.87 (-0.16)	-0.96 (-0.19)	-0.71	-0.79
d(Al-*O*/*N*) (Å)		1.83	1.97		
q_1q_2/d		-1.0316	-1.0039		

A second interaction likely contributes to the difference between BnOH and aniline. The coordination of the reactant and product molecules leads to decoordination of one or several O atoms of the initially κ^2-coordinated triflate anions from the Al(III) center. These O atoms can now participate in stabilizing H-bonds with protons from the molecules coordinated to Al(III) (Figure 5b-d). The strongest H-bonds are formed with O-bound molecules, *i.e.* BnOH (1 bond with *d*(O_{OTf}-H) = 1.50 Å) and water (2 bonds with *d*(O_{OTf}-H) = 1.59-1.60 Å), while much weaker bonds are formed with the N-containing aniline and *N*-phenyl benzylamine (*d*(O_{OTf}-H) = 1.84-2.03 Å).

The energetic gain of binding a second BnOH molecule to Al(OTf)$_3$(BnOH) is smaller (-58 kJ mol^{-1}, see Table S3, entry 5) than for the first molecule, probably because the Lewis acidity of Al(III) is reduced by the already bound BnOH. Note that for the other molecules, the relative binding strengths (i.e BnOH > aniline > H_2O) are preserved (Table S3, entries 6-7). The binding of a 3rd BnOH molecule on Al(III) results in a strong stabilization by -70 kJ mol^{-1} *vs.* Al(OTf)$_3$(BnOH)$_2$, probably because a very stable octahedral structure is formed (ΔG_{bind} = -215 kJ mol^{-1}, Figure 6a and Table S3, entry 8). Note that when only one type of molecule is coordinated, both *fac* and *mer* isomers can be formed with either all triflate ions and ligands grouped on opposite sides of the octahedron (*fac*), or occupying the octahedral planes (*mer*). The latter was found more stable than *fac*-coordination by 32, 51 and 14 kJ mol^{-1} for BnOH, aniline and water, respectively, most likely because steric and electrostatic repulsion between the coordinated molecules and the triflate anions is minimized (Table S3). The higher binding strength of BnOH, compared to aniline and water, is conserved for the binding of 3 molecules (ΔG_{bind} = -215 *vs.* -183 kJ mol^{-1} and -154 kJ mol^{-1}, respectively, see Figure 6a-c).

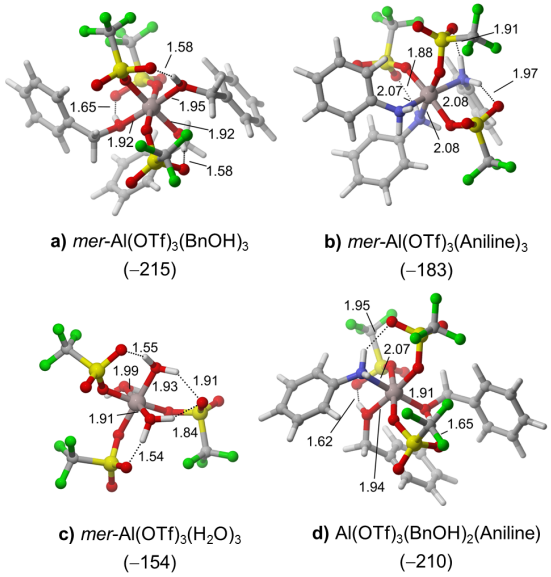

a) *mer*-Al(OTf)$_3$(BnOH)$_3$ (–215) **b)** *mer*-Al(OTf)$_3$(Aniline)$_3$ (–183)

c) *mer*-Al(OTf)$_3$(H$_2$O)$_3$ (–154) **d)** Al(OTf)$_3$(BnOH)$_2$(Aniline) (–210)

Figure 6. Selected optimized structures of complexes of Al(OTf)$_3$ with 3 molecules of BnOH, aniline, or water; and calculated binding free energies (ΔG_{bind} at 25 °C in toluene, kJ mol^{-1}, indicated in brackets).

We also calculated all possible mixed combinations with n BnOH / l aniline and m water molecules (n + l + m = max. 3, see Table S3). This analysis confirms that *mer*-Al(OTf)$_3$(BnOH)$_3$ is indeed the most stable structure in toluene, thus corroborating and

quantifying the experimental findings, which clearly indicated preferential binding of BnOH in toluene. BnOH is present in all most stable mixed configurations (see for example Figure 6d and Table S3, entries 8-12) and all combinations without BnOH are significantly less stable. The charge transfer (withdrawal of electrons) from the ligands to Al decreases with the number of ligands, going from +0.25 for 1 BnOH (see Table 2) to 0.24, and 0.15 for 2 and 3 BnOH, respectively (see Table S4). At the same time, the average bond length Al-*O*(H)$CH_2C_5H_5$ increases from 1.83 to 1.93 Å (see Table S4). Both factors are consistent with a decreasing binding energy per ligand (Figure S9a).

The binding free energies were in addition computed at 160 °C (reaction temperature) (Table S3, Figure S9b). As expected, at this temperature, binding to $Al(OTf)_3$ is much less favorable. Low-coordinated and potentially more reactive metastable complexes such as $Al(OTf)_3(BnOH)_2$ and $Al(OTf)_3(BnOH)$ are thus accessible under reaction conditions, but unlikely at 25 °C, at which CV and conductometry tests were performed. In what follows, $Al(OTf)_3(BnOH)_3$ is the most stable structure in toluene, *i.e.* the *resting* state of the catalyst, while less stable structures will be called *reactive* states.

Reaction mechanism

In polar solvents, a S_N1-type mechanism can be proposed for the direct amination reaction of BnOH. Indeed, dissociation of $Al(OTf)_3(BnOH)_3$ into $[Al(OTf)_3(BnOH)_2(OH)]^-$ and a benzyl cation is feasible in nitromethane, albeit associated with a sizeable barrier ($\Delta G^{\ddagger}$ = +97 kJ mol^{-1}). Combined with the energetic cost to displace the strongly bound aniline from the Al(III) center (vide *supra*), this explains why much harsher conditions are necessary than for the more reactive secondary alcohols, and less basic and thus less coordinating amine derivatives used by Mashima.[11b] The formation of cationic species is very likely responsible for side reactions and in turn for the low selectivity. In contrast, in toluene, where a S_N1 mechanism is impossible (ΔG = +272 kJ mol^{-1}), one can more reasonably assume a S_N2-type mechanism, in which aniline attacks the C-atom of BnOH coordinated to Al(III), thus avoiding the formation of ionic species.

Starting from $Al(OTf)_3(BnOH)_3$, three different C-O bonds can be broken. Since the structures of the transition states are similar, we only report the most favorable case (Figure 8a and Figure 9, $\Delta G^{\ddagger}$ = 117 kJ mol^{-1}; attack on the other two benzylic carbon atoms is slightly less favorable by 3 and 13 kJ mol^{-1}). The transition state features trigonal-bipyramidal coordination and sp^2-hybridization of carbon, as expected for a S_N2 reaction. The O-C-N angle formed between the breaking C-O and the forming C-N bond is close to linear (162°). Note, that a triflate ligand stabilizes the transition state by forming a H-bond with one of the protons of aniline. The product of an intrinsic reaction coordinate (IRC) run starting from the transition state converges to a stable structure in which protonated *N*-phenyl benzylamine is bound to $[Al(OTf)_3(BnOH)_2(OH)]^-$ (Figure 8b and Figure 9, ΔG = -21 kJ mol^{-1}). This structure can be interpreted either as an ion-pair, or as an acid-base adduct in which the basic N of the amine product interacts with the proton of the water molecule, which, in turn, is acidified by its coordination to Al(III). Proton transfer and decoordination of *N*-phenylbenzylamine leads to $Al(OTf)_3(BnOH)_2(H_2O)$ (ΔG = -1 kJ mol^{-1}), and release of water to $Al(OTf)_3(BnOH)_2$. Unlike the most stable isomer found for coordination of 2 BnOH (Table S3, entry 5), the resulting structure is five-coordinate and therefore less stable (ΔG = +70 kJ mol^{-1}). Finally, BnOH coordination leads back to $Al(OTf)_3(BnOH)_3$ (ΔG = -18 kJ mol^{-1}), the resting state of the catalyst.

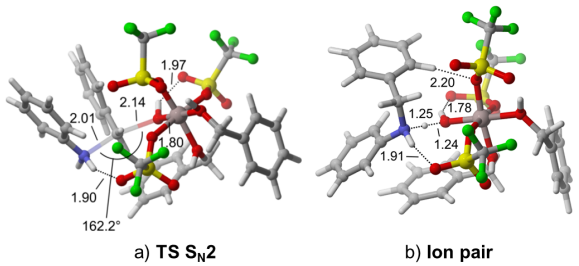

Figure 8. Transition state (TS S_N2) and ion-pair for the reaction of aniline with $Al(OTf)_3(BnOH)_3$ in toluene; selected distances are indicated in Å.

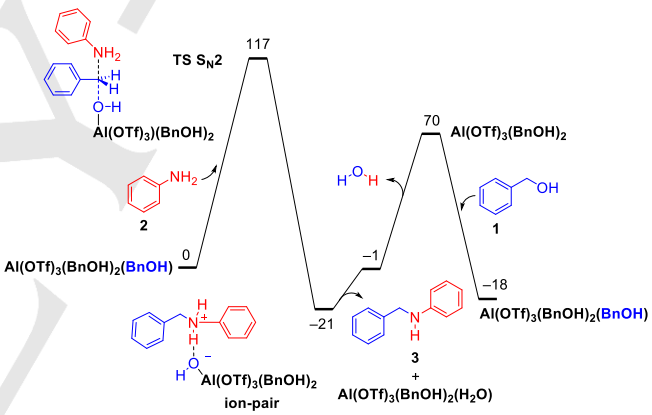

Figure 9. Calculated free energy profile for the direct amination of benzyl alcohol with aniline to *N*-phenylbenzylamine and water in toluene solvent. Free energies (ΔG at 160 °C, kJ mol^{-1}) are defined relative to separate $Al(OTf)_3(BnOH)_3$ and aniline.

Effect of coordinated species on the catalyst efficiency

In addition to $Al(OTf)_3(BnOH)_3$, the resting state of the catalyst (*i.e.* the most stable situation), we studied *reactive* states of the catalyst, *i.e.* less stable structures in which one or several BnOH have been exchanged by either aniline or water. The height of the intrinsic barrier ($\Delta G^{\ddagger}_{intr}$) provides a measure of the reactivity of each reactive state, while the total barrier ($\Delta G^{\ddagger}_{tot}$) compares the reactivity with that of $Al(OTf)_3(BnOH)_3$ (Table 3). For both $Al(OTf)_3(BnOH)_2(X)$ and $Al(OTf)_3(BnOH)(X)_2$ with X = H_2O or aniline, the structures of the transition state and ion-pairs (Figure S10a-d) are very similar to those found for $Al(OTf)_3(BnOH)_3$. As a result, the intrinsic barriers are similar (Table 3, entries 2-5) ($\Delta G^{\ddagger}_{intr}$ = 117 kJ mol^{-1}, Table 3, entry 1), while in the case of $Al(OTf)_3(BnOH)_2(H_2O)$ the barrier is even lower ($\Delta G^{\ddagger}_{intr}$ = +108 kJ mol^{-1}, Table 3, entry 3). This means that for coordination of 3 ligands to Al(III), the nature of the ligands has no significant

effect on the reactivity of coordinated BnOH. However, given the lower stability of the reactive states compared to $Al(OTf)_3(BnOH)_3$, the cost for ligand exchange has to be accounted for. Indeed, when only 1 BnOH is exchanged for aniline or water, the effect is small, ($\Delta G^{\ddagger}_{tot}$ = 121-123 kJ mol^{-1}, Table 3, entries 2-3), but when 2 ligands are exchanged, the reaction becomes significantly more difficult ($\Delta G^{\ddagger}_{tot}$ = 140-151 kJ mol^{-1}, Table 3, entries 4-5).

Table 3. Calculated intrinsic free energy barrier with respect to the reactive state ($\Delta G^{\ddagger}_{intr}$) and aniline, total free energy barrier ($\Delta G^{\ddagger}_{tot}$) with respect to the resting state $Al(OTf)_3(BnOH)_3$ and aniline, and partial charge on the Al atom calculated by NBO (difference *vs.* $Al(OTf)_3(BnOH)_3$ in brackets); free energies in toluene at 160 °C (kJ mol^{-1})

Entry	Reactive state	$\Delta G^{\ddagger}_{intr}$	$\Delta G^{\ddagger}_{tot}$	Charge on Al
1	$Al(OTf)_3(BnOH)_3$	117	117	2.09
2	$Al(OTf)_3(BnOH)_2$(Aniline)	117	121	2.06 (-0.03)
3	$Al(OTf)_3(BnOH)_2(H_2O)$	108	123	2.03 (-0.06)
4	$Al(OTf)_3(BnOH)(Aniline)_2$	119	140	2.05 (-0.04)
5	$Al(OTf)_3(BnOH)(H_2O)_2$	119	151	2.01 (-0.08)
6	$Al(OTf)_3(BnOH)$	71	155	2.17 (+0.08)

Finally, we also studied the reactivity of the low-coordinated complex $Al(OTf)_3(BnOH)$. Not surprisingly, the energy barrier for the S_N2 reaction is very low ($\Delta G^{\ddagger}_{intr}$ = 71 kJ mol^{-1}, Figure S10e), most likely because of its higher Lewis acidity, as apparent from the higher partial charge on Al(III) compared to coordination by 3 ligands (Table 3, last column). However, as already mentioned, starting from $Al(OTf)_3(BnOH)_3$, the formation of $Al(OTf)_3(BnOH)_2$ and $Al(OTf)_3(BnOH)$ by successive losses of BnOH is associated with an energetic cost of 55 and 29 kJ mol^{-1}, respectively (Table S3, entries 1, 5, and 8). Overall, the energetic cost to generate $Al(OTf)_3(BnOH)$ outweighs its higher reactivity, leading to an overall barrier of $\Delta G^{\ddagger}_{tot}$ = 155 kJ mol^{-1} (Table 3, entry 6), which is significantly higher than that for the fully coordinated resting state of the catalyst, or other reactive states. It is therefore unlikely that the low-coordinated complex $Al(OTf)_3(BnOH)$ contributes to the observed reactivity.

Conclusion

We have successfully extended the $Al(OTf)_3$-catalyzed direct amination of activated secondary alcohols with electron-poor amine derivatives[11b] to activated primary alcohols and electron-rich amines, by studying the model reaction of benzyl alcohol (BnOH) an aniline. By combining experiments with DFT simulations, we were able to provide detailed insight into the structure of the catalyst and the mechanism of the reaction, which were found to strongly depend on the type of solvent (polar *vs*. non-polar). Competition between aniline and benzyl alcohol was evidenced both by NMR spectroscopy and cyclic voltammetry, and proved to be critical to explain how the solvent conditions the reactivity. The strong affinity of aniline for Al(III) in nitromethane solvent, which can be attributed to the formation of ionic species, is responsible for catalyst deactivation and very low selectivity. Under such conditions, a S_N1-type mechanism is active. In contrast, in toluene, the reaction is very selective, leading to almost exclusive formation of the desired N-phenylbenzylamine. In this case, competition of BnOH and aniline for Al(III) binding is in favor of BnOH, as shown experimentally and validated by DFT calculations, predicting the formation of $Al(OTf)_3(BnOH)_3$ as the most stable complex (resting state of the catalyst). The calculations strongly support a S_N2 mechanism in which aniline attacks the C-atom of BnOH coordinated to Al(III), thus avoiding the formation of ionic species, and leading to much higher selectivity. To our knowledge, it is the first time that such type of mechanism is proposed for metal triflate-catalyzed substitution reactions. Also, instead of a single active species, as commonly assumed in homogeneous catalysis, we find that several species, generated by exchange of coordinated BnOH with water or aniline, can be active. Further investigations about how the solvent, reactants and products condition the reactivity of metal triflates are currently underway in our laboratories.

Acknowledgements

The authors would like to express their gratitude to Solvay, CNRS, PSL, ENS Paris, ENS de Lyon,UPMC and UCLA for funding. P.A. Payard is grateful to ENS Paris Saclay for a PhD grant. J. Lai (E2P2L) is acknowledged for useful discussions.

Keywords: Amination • Alcohol • Aluminum Triflate • Nucleophilic Substitution • DFT• Homogeneous Catalysis

[1] (a) H. A. Wittcoff, B. G. Reuben, J. S. Plotkin, *Industrial Organic Chemicals*, 2nd ed., Wiley, NY, **2004**; (b) S. A. Lawrence, *Amines: Synthesis Properties and Applications*, Cambridge University: Cambridge, **2004**; (c) B. R. Brown, *The Organic Chemistry of Aliphatic Nitrogen Compounds*, Cambridge University: Cambridge, **2004**.

[2] (a) E. Emer, R. Sinisi, M. G. Capdevila, D. Petruzziello, F. De Vincentiis, P. G. Cozzi, *Eur. J. Org. Chem.* **2011**, *2011*, 647-666; (b) M. Pera-Titus, F. Shi, *ChemSusChem* **2014**, *7*, 720-722; (c) S. Bähn, S. Imm, L. Neubert, M. Zhang, H. Neumann, M. Beller, *ChemCatChem* **2011**, *3*, 1853-1864; (d) A. Baeza, C. Nájera, *Synthesis* **2014**, *46*, 25-34.

[3] B. Trost, *Science* **1991**, *254*, 1471-1477.

[4] (a) T. D. Nixon, M. K. Whittlesey, J. M. J. Williams, *Dalton Trans.* **2009**, 753-762; (b) G. Guillena, D. J. Ramón, M. Yus, *Chem. Rev.* **2010**, *110*, 1611-1641; (c) J. L. Klinkenberg, J. F. Hartwig, *Angew. Chem. Int. Ed.* **2011**, *50*, 86-95; (d) C. Gunanathan, D. Milstein, *Science* **2013**, *341,* 1229712; (e) Q. Yang, Q. Wang, Z. Yu, *Chem. Soc. Rev.* **2015**, *44*, 2305-2329.

[5] J. Neumann, S. Elangovan, A. Spannenberg, K. Junge, M. Beller, *Chem. Eur. J.* **2017**, *23*, 5410-5413.

[6] B. Emayavaramban, M. Roy, B. Sundararaju, *Chem. Eur. J.* **2016**, *22*, 3952-3955.

[7] (a) H. Bricout, J.-F. Carpentier, A. Mortreux, *J. Mol. Cat. A: Chem* **1998**, *136*, 243-251; (b) Y. Gumrukcu, B. de Bruin, J. N. H. Reek, *Catalysts* **2015**, *5*, 349-365; (c) S. Sawadjoon, P. J. R. Sjoberg, A. Orthaber, O. Matsson, J. S. M. Samec, *Chem. Eur. J.* **2014**, *20*, 1520-1524; (d) J. Muzart, *Eur. J. Org. Chem.* **2007**, *2007*, 3077-3089.

[8] (a) H. Bricout, J.-F. Carpentier, A. Mortreux, *Tetrahedron* **1998**, *54*, 1073-1084; (b) Y. Kita, H. Sakaguchi, Y. Hoshimoto, D. Nakauchi, Y. Nakahara, J.-F. Carpentier, S. Ogoshi, K. Mashima, *Chem. Eur. J.* **2015**, *21*, 14571-14578.

[9] J.-F. Gal, C. Iacobucci, I. Monfardini, L. Massi, E. Duñach, S. Olivero, *J. Phys. Org. Chem.* **2013**, *26*, 87-97.

[10] S. Haubenreisser, M. Niggemann, *Adv. Synth. Catal.* **2011**, *353*, 469-474.

[11] (a) M. Gohain, C. Marais, B. C. B. Bezuidenhoudt, *Tetrahedron Lett.* **2012**, *53*, 1048-1050; (b) T. Ohshima, J. Ipposhi, Y. Nakahara, R. Shibuya, K. Mashima, *Adv. Synth. Catal.* **2012**, *354*, 2447-2452.

[12] J.-M. Yang, R. Jiang, L. Wu, X.-P. Xu, S.-Y. Wang, S.-J. Ji, *Tetrahedron* **2013**, *69*, 7988-7994.

[13] (a) W. Huang, Q.-S. Shen, J.-L. Wang, X.-G. Zhou, *Chin. J. Chem.* **2008**, *26*, 729-735; (b) W. Rao, X. Zhang, E. M. L. Sze, P. W. H. Chan, *J. Org. Chem.* **2009**, *74*, 1740-1743; (c) M. Noji, T. Ohno, K. Fuji, N. Futaba, H. Tajima, K. Ishii, *J. Org. Chem.* **2003**, *68*, 9340-9347.

[14] (a) R. Jiang, C.-X. Yuan, X.-P. Xu, S.-J. Ji, *Appl. Organomet. Chem.* **2012**, *26*, 62-66; (b) H. Qin, N. Yamagiwa, S. Matsunaga, M. Shibasaki, *Angew. Chem. Int. Ed.* **2007**, *46*, 409-413.

[15] W. Rao, P. Kothandaraman, C. B. Koh, P. W. H. Chan, *Adv. Synth. Catal.* **2010**, *352*, 2521-2530.

[16] (a) X. Giner, P. Trillo, C. Nájera, *J. Organomet. Chem.* **2011**, *696*, 357-361; (b) B. Sreedhar, P. Surendra Reddy, M. Amarnath Reddy, B. Neelima, R. Arundhathi, *Tetrahedron Lett.* **2007**, *48*, 8174-8177.

[17] H. Yamamoto, E. Ho, I. Sasaki, M. Mitsutake, Y. Takagi, H. Imagawa, M. Nishizawa, *Eur. J. Org. Chem.* **2011**, *2011*, 2417-2420.

[18] (a) V. Terrasson, S. Marque, M. Georgy, J.-M. Campagne, D. Prim, *Adv. Synth. Catal.* **2006**, *348*, 2063-2067; (b) H. Hikawa, H. Suzuki, Y. Yokoyama, I. Azumaya, *J. Org. Chem.* **2013**, *78*, 6714-6720; (c) T. Ohshima, Y. Nakahara, J. Ipposhi, Y. Miyamoto, K. Mashima, *Chem. Commun.* **2011**, *47*, 8322-8324; (d) B. Biannic, A. Aponick, *Eur. J. Org. Chem.* **2011**, *2011*, 6605-6617; (e) M. Georgy, V. Boucard, O. Debleds, C. D. Zotto, J.-M. Campagne, *Tetrahedron* **2009**, *65*, 1758-1766.

[19] P. Trillo, A. Baeza, C. Nájera, *Eur. J. Org. Chem.* **2012**, *2012*, 2929-2934.

[20] (a) J.-F. Gal, C. Iacobucci, I. Monfardini, L. Massi, E. Duñach, S. Olivero, *J. Am. Soc. Mass. Spectrom.* **2012**, *23*, 2059-2062; (b) G. Compain, L. Sikk, L. Massi, J. F. Gal, E. Dunach, *ChemPhysChem* **2017**, *18*, 683-691; (c) C. Iacobucci, N. Jouini, L. Massi, S. Olivero, F. De Angelis, E. Duñach, J.-F. Gal, *ChemPlusChem* **2017**, *82*, 498-506; (d) I. Monfardini, L. Massi, E. Dunach, S. Olivero, J.-F. Gal, *Chem. Commun.* **2010**, *46*, 8472-8474.

[21] Y. Koito, K. Nakajima, H. Kobayashi, R. Hasegawa, M. Kitano, M. Hara, *Chem. Eur. J.* **2014**, *20*, 8068-8075.

[22] (a) L. Coulombel, M. Rajzmann, J.-M. Pons, S. Olivero, E. Duñach, *Chem. Eur. J.* **2006**, *12*, 6356-6365; (b) Z. Li, R. S. Assary, A. C. Atesin, L. A. Curtiss, T. J. Marks, *J. Am. Chem. Soc.* **2013**, *136*, 104-107.

[23] R. S. Assary, A. C. Atesin, Z. Li, L. A. Curtiss, T. J. Marks, *ACS Catal.* **2013**, *3*, 1908-1914.

[24] A. Jutand, *Chem. Rev.* **2008**, *108*, 2300-2347.

[25] The presence of adventitious water in the experiment can be due either to the commercially available nitromethane (98.5% purity, kept on molecular sieves (3 Å)) and to the hygroscopy of aluminum triflate (kept under vacuum on anhydrous P_2O_5)

[26] Comparable shifts due to the formation of alcohol-Al$(OTf)_3$ complexes were observed by Dunach and collaborators in the mecanistic study of the hydroalkoxylation of unactivated olefins, see ref [22a]

[27] In low polar solvents, the use of ultramicroelectrodes is mandatory due to ohmic drop issues, see : C. Amatore, F. Pluger, *Organometallics* **1990**, *9*, 2276-2282.

[28] K. P. Kepp, *Inorg. Chem.* **2016**, *55*, 9461-9470.

[29] (a) J. P. Foster, F. Weinhold, *J. Am. Chem. Soc.* **1980**, *102*, 7211-7218; (b) A. E. Reed, L. A. Curtiss, F. Weinhold, *Chem. Rev.* **1988**, *88*, 899-926.

FULL PAPER

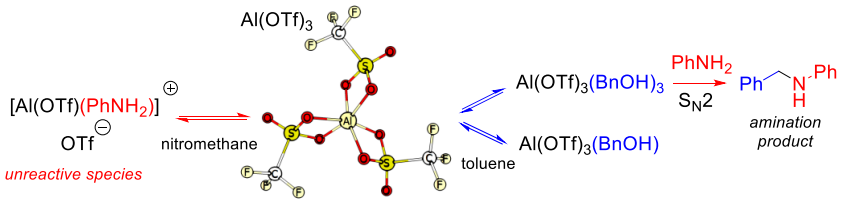

The use of aluminum triflate, $Al(OTf)_3$ as catalyst for the direct amination of activated primary alcohols with electron-rich amines is reported. Competition between aniline and benzyl alcohol is evidenced both by NMR spectroscopy and cyclic voltammetry, and is shown to be critical to explain how the solvent conditions the reactivity in polar and non-polar solvents, with a high selectivity in toluene. Density functional theory (DFT) calculations rationalize the impact of the catalyst structure on the reactivity, and support an unprecedented S_N2-type mechanism in toluene.

Pierre-Adrien Payard, Qingyi Gu, Wenping Guo, Qianran Wang, Matthieu Corbet, Carine Michel, Philippe Sautet, Laurence Grimaud, Raphael Wischert, and Marc Pera-Titus**

Page No. – Page No.

Direct Amination of Alcohols Catalyzed by Aluminum Triflate: an Experimental and Computational Study